WEB OF SCIENTIST: INTERNATIONAL SCIENTIFIC RESEARCH JOURNAL
ISSN: 2776-0979, Volume 3, Issue 7, July, 2022

# UNDERSTANDING THE MAGNETO CALORIC EFFECT IN SUPER SPIN GLASS COBALT-BASED NANOPARTICLES

Jo'lanov Hasan Komilovich
Department of Coordination of Joint Educational Programs with Samarkand Higher Education Institutions of the Samarkand Institute of Economics and Service, Samarkand 140104, Uzbekistan

Azimov Alisher Mirzo ugli
Department of Coordination of Joint Educational Programs with Samarkand Higher Education Institutions of the Samarkand Institute of Economics and Service, Samarkand 140104, Uzbekistan

Omadjon Safarov
Department of Solid State Physics, Faculty of Physics, Samarkand State University, Samarkand 140104, Uzbekistan

Abdiev Jurabek Muzaffar ugli
Physical-Technical Institute SPA "Physics-Sun", Uzbek Academy of Sciences, 100084, Tashkent, Uzbekistan

Yaxshimurodov Ahmad Asror ugli
Teacher of Physics at the 16th General Education School Under the Public Education Department of Pasdargom District of Samarkand Region

## Abstract

The magneto caloric effect has been investigated in bimetallic Co/Au (core/shell) nanoparticles system exhibiting magnetic transition and non-equilibrium spin dynamics at low temperatures. The analysis of system's magneto caloric properties by means of Maxwell relations application to both isothermal and zero field cooling magnetization data has been performed. Peaks of magnetic entropy change vs. temperature dependences ($\Delta s_M(T)$) have been observed at a temperature in the vicinity of the magnetic transition. Despite of significant thermal hysteresis of magnetization at low applied fields a master curve has been constructed from the $\Delta s_M(T)$dependences employing scaling analysis that confirms the investigated transition is of the second order type. Different values of critical exponents calculated from field dependence of relevant magneto

caloric response parameters in the proximity of critical temperature have been found for low and high applied fields. Along with the unique feature of Co/Au (core/shell) nanoparticle systems, where the working temperature of the potential refrigerant can be tuned easily by particles size change, this kind of system appears promising candidate for the future cryogenic magnetic refrigeration applications.

**Keywords:** Magnetic nanoparticles, Magneto caloric effect, Magnetic transition, Scaling analysis, Cryogenic applications

## Introduction

Despite of intensive research on nanostructures driven mainly by the high application potential of these kind of materials in a variety of disciplines like medicine [1,2], techniques [3], or industry [4,5], only a few works devoted to examination of magnetic nanoparticles (NPs) with respect to their magneto caloric properties have been reported so far [6e9]. The magneto caloric effect (MCE) refers to conversion of magnetic energy of a magnetic substance into thermal energy under applying or removing an external magnetic field under adiabatic condition [10]. Since the effect is known over a century, it has been a fundament for several magnetic refrigeration techniques and a number of feasible refrigerant materials that have already been designed [11]. Large magnetic entropy change has been reported for MnFeP0.45As0.55 compound [12], which contrary to another feasible material Gd5(Si2Ge2) exhibiting so-called giant MCE-effect [13], allows magnetic refrigeration even at room temperature. In both cases, magneto- structural phase transition has been attributed to the root cause of the observed phenomenon. Heusler alloys are also known for their hallmarks of MCE. The study on influence of compositional variations induced by the small changes in concentrations of the components conducted on magneto caloric properties of numerous NiMn-based compounds is available elsewhere [14]. Yet another group of materials have been found interesting from MCE application point of view. Recently, Arial et al. [15] reported works dealing with the MnCoGe compounds that belong to the family of materials undergoing magneto-structural phase transition. By means of partial doping Ag or Al on Mn sites they induced structural changes leading to observation of large values of

magnetic entropy change (up to 22 J/kgK for field change 5 T) near room temperatures.

In the process of tailoring the qualities of potential refrigerants, magnetic nanoparticles have been found very promising. The main advantage of nanoparticles over the bulk materials stems from wider options for tuning the characteristics of the refrigerant material. Since the change of working temperature, refrigeration capacity or phase transition character in bulk materials can be induced almost exclusively by chemical composition, in the case of NPs size, shapes, capping layer or dilution of nanoparticle system affect those features considerably. Monte Carlo simulations carried out by Baldomir et al. [16] suggest that for a given sample con- centration of superparamagnetic NPs there exists a particle size that provides larger entropy increase, and reciprocally for a given particle volume there exists a sample concentration allowing producing larger entropy change. Significantly different behavior was documented by Phan et al. [17] in the bulk and nanostructured (50 nm and 35 nm) gadolinium iron garnets $Gd_3Fe_5O_{12}$. While the peak of magnetic entropy change $\Delta s_M(T)$ in bulk sample was found almost independent of the applied magnetic field, the ones corresponding to nanostructured samples tended to shift towards lower temperatures as the applied magnetic field was increased. More- over, an increase in the magnitude of $\Delta s_M(T)$ was documented with diminishing particle size. The authors ascribed this feature to sur- face spin disorder in nanostructured samples. Hueso et al. [9] studied MCE properties of $La2/3Ca1/3MnO_3$ nanoparticles and found out that the first-order magnetic transition can be minimized and eventually evolves towards a second-order one as the grain size diminishes. Thus, we are able to change the nature of an intrinsic property of a material by changing the particle size. The investigations of numerous bulk systems exhibiting MCE by means of scaling analysis show that in the case of the materials undergoing the second order phase transition (SOPT) an universal curve can be constructed from the magnetic entropy change vs. temperature dependences after proper rescaling [18,19]. Therefore, the collapse of $\Delta s_M(T)$ curves can be regarded as the relevant indicator of SOPT in bulk crystalline and amorphous alloys [20e23]. Franco et al. [24] extended this kind of analysis to monodispersed core/shell Co, Co/ Ag and Ni/Ag nanoparticle systems. They utilized the field dependence of the magnetic entropy change peak for the surface spin freezing transition study and concluded that although the magnitude of entropy change peak and

position of the peak can be tuned by changing the composition and nature (metallic or organic) of the shell and surfactant layers, the characteristics of the spin freezing transition are not altered.

Apparently, there is a need for extended investigation of many interesting phenomena inherent to magnetic NPs, such as the influence of particle shape, size, concentration, surface effects or interparticle interactions on MCE. Even though some pioneering works dealing with these problems have already been published, tremendous variability of nanoparticle and nanocomposite systems deserves extensive investigation in order to reveal fundamental laws with all of their peculiarities. Hence, we decided to prepare a monodisperse core/shell Co/Au nanoparticle system and study its magneto caloric properties. As it was demonstrated elsewhere [25], this system exhibits features of non-equilibrium dynamics induced by strong inter-particle interactions what lead to formation of super spin glass state. This work is the first attempt to apply scaling analysis of $\Delta s_M(T)$[18] developed for bulk materials on nanoparticle system exhibiting super spin glass state in order to examine the characteristics of the phase transition. Since complex study on MCE characteristics of similar system has not been reported yet, we put forward our results of magnetic entropy change, field dependence of relevant MCE parameters, scaling analysis and critical exponents obtained by processing the experimental data.

## Experimental

Examined Co/Au nanoparticles were synthesized employing the reverse micelle method. Studied nanoparticles were prepared via micro emulsion method and reverse micelle solutions were prepared using CTAB as the surfactant, with octane as the oil phase, 1-butanol as co-surfactant, and aqueous reactants of $CoCl_2$, $NaBH_4$, and $HAuCl_4$. As a first, the blank Co core was prepared inside reverse micelle solution and the size of Co core was controlled by the water to surfactant molar ratio $W = [H_2O]/[CTAB]$ 8. Subsequently, the coating of Au shell was coated also using the reverse micelle method, and the size of shell by the water to surfactant molar ratio w $W = [H_2O]/[CTAB] = 5$ was controlled. The determined method allowed us to prepare nanoparticles with Co magnetic core with a size of about 5e7 nm coated with an Au diamagnetic shell with a thickness of about 2e3 nm. Utilized chemicals, process of preparation, particles' structural analysis via X-ray diffraction and high resolution transmit ion electron microscopy along

with histogram of particles' size distribution can be found elsewhere [25]. Monodisperse core/shell nanoparticle system (denoted as Co/Au1 in Ref. [25]) exhibited average particle's magnetic moment 86 $\mu_B$. The analysis of AC magnetic susceptibility data revealed the presence of non- equilibrium dynamics and freezing of the nanoparticles' magnetic moments into the super spin glass state at $T_{SSG}$ ~7 K. The morphology of the investigated system, displayed in Fig. 1, was studied using a JEOL 2100F microscope and the bright-field TEM images were obtained at 200 kV. Studied nanoparticles are homogenous, spherical shaped, and the size distribution obtained from the TEM images confirmed the average particles diameter $d_{TEM}$ ~7 nm.

Magnetic properties of the system were examined by SQUID- based magnetometer (Quantum Design MPMS 5XL). The powder sample with 18 mg mass was put into the bottom of the gelatin capsule cap, where it was fixed by the reversed body of the capsule in order to prevent its movement. Subsequently, it was placed into a plastic holder. The signal of the empty capsule and holder was measured and subtracted from experimental data.

Zero-field-cooling $M^{ZFC}$ and field-cooling $M^{FC}$ measurements were carried out in temperature range 1.8e30 K in applied fields up to 1 T. $M^{ZFC}$ process refers to cooling the sample with the absence of external magnetic field to desired temperature. Afterwards, certain field was applied and the magnetization data was collected while heating the sample. According to $M^{FC}$ protocol, the sample was exposed to constant magnetic field at high temperature and magnetization was taken with decreasing temperature.

Isothermal magnetization curves were obtained using the following protocol which is based on standard protocol commonly being used for M(H) data collection [26,27]. The sample was cooled down in zero magnetic field to 20.8 K and subsequently isothermal magnetization curves M(H) were recorded in a temperature range from 20.8 to 1.8 K with a step of 0.5 K in applied fields up to 5 T. Unlike in the standard protocol, we collected the M(H) data with decreasing temperature. For further analysis, we account only the data obtained at applied fields higher than 1T where the presence of thermal hysteresis can be ruled out (evidence provided by $M^{ZFC}/M^{FC}$measurements). We assume, this approach renders better consistence with $M^{FC}$ data set which has been chosen for fundamental analysis and evaluation in this work.

WEB OF SCIENTIST: INTERNATIONAL SCIENTIFIC RESEARCH JOURNAL
ISSN: 2776-0979, Volume 3, Issue 7, July, 2022

MCE was examined by means of magnetic entropy change vs. temperature dependences calculated from $M^{ZFC}$ and $M^{FC}$ and isothermal magnetization data for low and high applied fields, respectively.

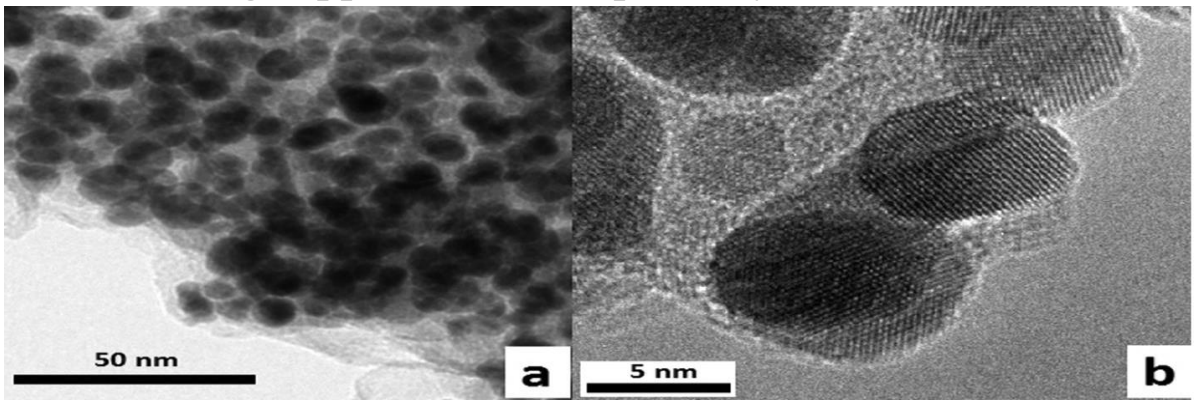


Fig. 1. TEM micrographs of (a) Co/Au nanoparticle assembly and (b) detail of selected area.

## Results and Discussion

### 1.1. DC magnetic measurements

Isothermal magnetization data recorded by means of protocol described in section 2, Fig. 2 (a), indicate expected dependence of investigated Co/Au nanoparticle system magnetization on applied field magnitude. For each fixed temperature, the magnetization rises with increasing applied field, and for the corresponding applied field magnitude, it decreases with diminishing temperature. This behavior is typical of super paramagnetic particles and it was documented in a host of similar systems [28,29].

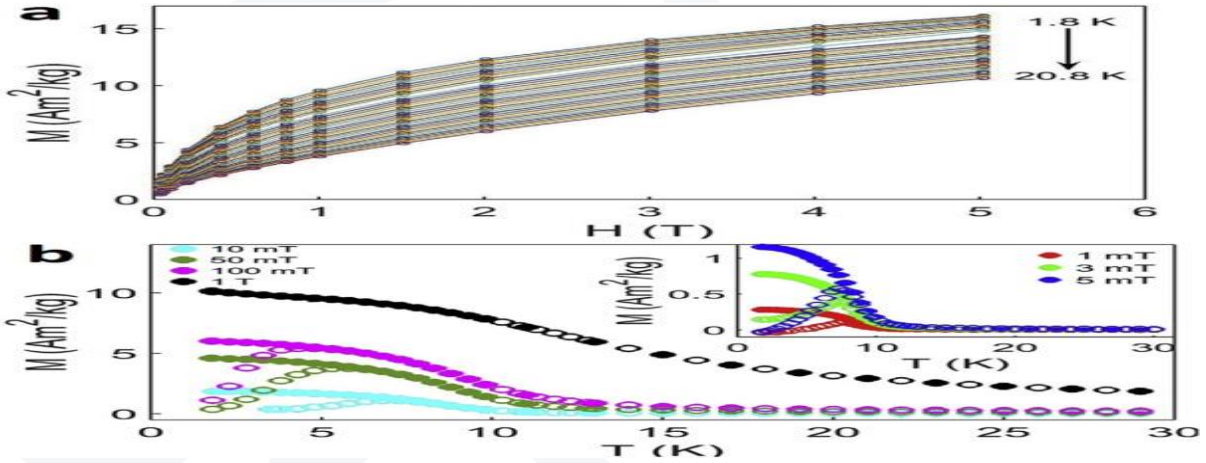


Fig. 2. (a) Isothermal magnetization data of investigated Co/Au nanoparticle system recorded with the step of 0.5 K in applied fields up to 5 T. (b) $M^{ZFC}$ (open symbols) and $M^{FC}$ (filled symbols) magnetization vs. temperature dependence of the Co/Au system obtained at constant applied

magnetic fields up to 1 T. 0.01e1 T. Data obtained at low fields 1e5 mT are shown in the inset.

At high temperature, where no restrictions with respect to magnetic moments of individual particles orientations are supposed, magnetization of the system can be described by well known Curie-Weiss or Langevin paramagnetic laws, where M ~ H/T. In the case of low temperatures, moments are either blocked in magnetization easy axis directions of NPs (display hallmarks of ferromagnetism) or, if inter particle interactions are strong enough, even frozen in super- spin glass state. However, both of the states, although obeying different laws, also follow fundamental dependence M ~ H/T. The deviations have been observed only in the systems with very strong inter particle interactions, where $M^{FC}$ has been found independent on temperature [30].

Fig. 2 (b) represents isofield magnetization data, where $M^{ZFC}$ curves exhibit field dependent single maximum at peak temperature ($T_P$) which shifts towards lower temperatures with the applied field increment up to 100 mT. This feature is typical of super paramagnetic NPs and according to Tadic [28,29], the peak temperature, $T_p$, $T_P$ can be attributed to experimental blocking temperature of the system at particular field. Decreasing the temperature below $T_P$ $M^{ZFC}$ and $M^{FC}$ curves start to bifurcate and significant thermal hysteresis becomes evident. The flat character of the $M^{FC}$ curve with tendency to saturate as it approaches the lowest temperatures is one of the characteristic features of super spin glass systems with no equilibrium dynamics, where strong inter particle interactions are dominant [31]. On the other hand, no thermal hysteresis was observed for $M^{ZFC}/M^{FC}$ curves obtained at $\mu_0 H = 1T$. These curves merge in the whole temperature span, suggesting that applied field was strong enough to overcome mutual interactions between particles and aligned the particles' magnetic moments even at the lowest temperatures.

In order to examine magneto caloric properties of the system via magnetic entropy change calculation, isothermal magnetization data obtained by means of standard protocol [26,27] are commonly being used in the majority of cases. However, it has been shown [31e33], that in the systems undergoing first order phase transition where thermal hysteresis is present, the application of Maxwell relation to the M(H) curves could possibly give unphysical magnetic entropy change spikes. This effect usually occurs if i) the

material is not properly prepared before each measurement (i.e. the memory of the sample is not properly erased) or ii) if the temperature interval between adjacent isotherms is lower than the extent of hysteresis. With the aim to suppress this feature, magnetization vs. temperature of the sample can be recorded at different constant magnetic fields and $\Delta s_M(T)$can be calculated from this data set avoiding artifacts [32,33]. Since ZFC/FC protocol meets the demand, we employed $M^{FC}$ and also $M^{ZFC}$ data for $\Delta s_M(T)$determination in the region of applied fields up to 1 T, where thermal hysteresis in the studied Co/Au system was observed.

The relationship between the change in magnetization and entropy can be expressed by Maxwell relation [34] $\mu_0(\partial M/\partial T)_H = (\partial S/\partial H)_T$ which for an isothermal-isobaric process after numerical approximated integration yields [35].

$$\Delta S_M\left(\frac{T_{n+1}+T_n}{2}, H_{\iota_{max}}\right) = \mu_0 \sum_{i=1}^{\iota max} \frac{(M_{n+1}-M_n)}{T_{n+1}-T_n}(H_{i+1}-H_i) \quad (1)$$

Susceptibility measurements in our previous work [25]. In addition, evaluation (discussed later) of M(H) data, Fig. 2 (a), obtained for high applied field region confirmed the presence of $\Delta s_M(T)$peak at T 7.5 K, thus at the very proximity of $T_{SSG}$ and close to $T_C$

Further study of our Co/Au system [37] by means of heat capacity measurements at applied fields of magnitudes from 1 to 9 T enabled independent determination of $\Delta S_M$ (T) values by different methods. As can be seen in Table 1, magnetic entropy change magnitude at peek point $\left|\Delta S_M^{pk}\right| = 0.89\,{}^{J}/_{kgK}$ established for the field change from 0 to 1 T is in rather good accordance with the value reported in present study.

Finally, we compared our results with the values reported by other authors for selected nanoparticle systems. The magnitudes of magnetic entropy change at corresponding critical temperatures $T_C$ where $M_n$ and ($M_{n+1}$ are the magnetization values measured in magnetic field $H_i$ at temperatures $T_n$ and $T_{n+1}$, respectively.

Fig. 3 presents magnetic entropy change vs. temperature dependences calculated from the experimental $M^{FC}$ data. In accordance with Maxwell relation, the slope of M(T) curves determines the quantity and the sign of magnetic entropy change, while the peaks of $\Delta s_M(T)$the occurrence of inflection points of $M^{FC}$ or $M^{ZFC}$ data. These inflection points are present in all right shoulders ($T > T_p$) of $M^{ZFC}$ curves and they are identical to the $M^{FC}$

ones, because the irreversibility does not emerge down to vicinity of $T_p$. However, in the case of left shoulders ($T < T_p$), inflection points of $M^{ZFC}$ follow the shift of $T_p$ towards lower temperatures with applied field increment and for the highest fields (100 mT, 1 T) do not even occur. Moreover, positive slope of $M^{ZFC}$ below $T_p$ could reflect the presence of inverse MCE in Co/Au nanoparticle system. Such behavior has been observed and described by Gorsse et al. [36] in $Tb_{60}Ni_{30}Al_{10}$ amorphous alloy exhibiting spin glass behavior and its examination is beyond the scope of this study.

Since MCE refers to the reversible temperature change under the application or removal of an external magnetic field under adiabatic condition and $M^{ZFC}$ data are not reversible under magnetic field cycling treatment, we utilized $M^{FC}$ data for $\Delta s_M(T)$ estimation, Fig. 3. As expected, processed data were found in agreement with results established from $M^{ZFC}$ curves above $T_p$ (curves not shown), where the positions of corresponding $\Delta s_M(T)$peaks (conventionally denoted as critical temperature $T_C$ [24), $T_C \sim 9$ K, along with their magnitudes were altered insignificantly. At this point, it is worth to emphasize good correlation of $\Delta s_M(T)$peaks' positions with freezing temperature of Co/Au nanoparticles' super spins $T_{SSG} \sim 7$ K established for the system from AC in applied field of 1 T are listed in Table 1.

### 1.2. Scaling Analysis

Numerous studies [11,18,23,24] showed that the occurrence of $\Delta s_M(T)$ peak. $\Delta S_M^{pk}(T)$ at peak temperature $T^{pk}$ can indicate magnetic phase transition in a system and analysis of the peak features can provide us with information on the character of possible phase transition [19], presence of minor phases in material [21] or system critical behavior [18]. In this study, we focused on the evaluation of $-\Delta s_M(T)$ peaks at the temperature $T > T_p$ and investigation of the characteristics of super paramagnetic to super spin glass state transition in the Co/Au nanoparticle system. With this objective we applied $\Delta s_M(T)$ scaling analysis proposed and experimentally verified for the systems undergoing the second order phase transition (SOPT) in bulk materials [18].

According to Franco et al. [18] $\Delta s_M(T, H)$ curves obtained for SOPT material can be rescaled onto a single curve which does not depend on field and in which the different temperature dependences are unified. The first step in constructing process of such master curve stems in identifying reference

WEB OF SCIENTIST: INTERNATIONAL SCIENTIFIC RESEARCH JOURNAL
ISSN: 2776-0979, Volume 3, Issue 7, July, 2022

temperature, $T_n$ for each $\Delta s_M(T)$ dependence. Reference temperature corresponds to a certain value of magnetic entropy change and it is identified as$\Delta s_M\ (T_r) = \varepsilon \Delta S_M^{pk}(T)$ , where ε is arbitrary selected real number be- tween 0 and 1. The value of ε = 0.5 was set for this study as it is the value commonly used for the purpose of scaling analysis [21,23,24]. Afterwards, $\Delta s_M(T)$ curves are normalized with respect to their maximum and finally the temperature axis is rescaled according to equation [21]. where $T_{r1}$ and $T_{r2}$ correspond to the reference temperatures below and above the $T^{PK}$ respectively.

Table 1 Magnetic entropy change magnitudes at peek point j$\Delta S^{pk}$j, critical temperatures (T )and refrigerant capacities (RC) of selected nanoparticle systems in applied field 1 T.

| | $T_C$ (K) | j$DS^{pk}$j (J/kgK) | RC (J/kg) |
|---|---|---|---|
| Co/Au nanoparticles | 9 | 0.7 | 4.49 |
| Co/Au nanoparticles | 9.55 | 0.89 | e |
| Co nanoparticles | 13 | 0.91 | e |
| Co/Ag nanoparticles | 13 | 0.89 | e |
| $La_{0.8}Ca_{0.2}MnO_3$ (17 nm)[e] | 90 | 0.1 | 20 |
| $La_{0.8}Ca_{0.2}MnO_3$ (28 nm)[e] | 210 | 1 | 75 |
| $La_{0.8}Ca_{0.2}MnO_3$ (43 nm)[e] | 236 | 4.2 | 40 |
| $La_{2/3}Ca_{1/3}MnO_3$ (60 nm)[e] | 260 | 0.5 | e |
| $La_{2/3}Ca_{1/3}MnO_3$ (500 nm)[e] | 260 | 5 | e |
| $CoFe_2O_4$ [f] | 223 | $2.5 \times 10^{-2}$ | e |

.

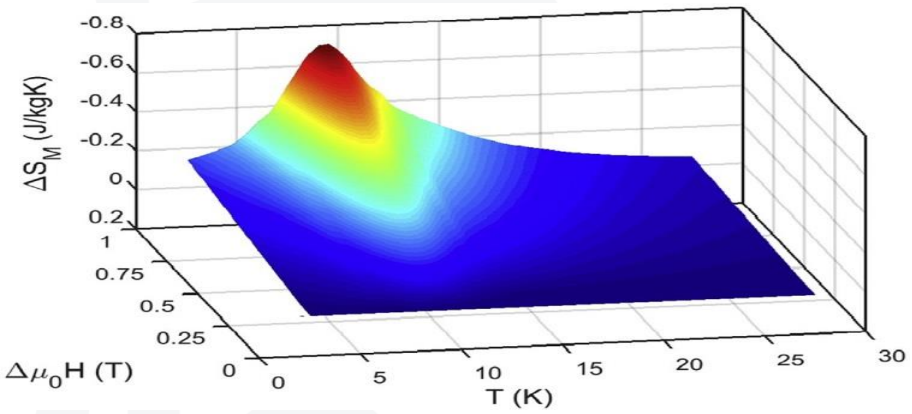


Fig. 3. Magnetic entropy change dependence on temperature of Co/Au system calcu lated from experimental $M^{FC}$ data for magnetic field variations up to 1 T.

[a] This study
[b] Co/Au system examined utilizing heat capacity measurements [37].

[c] Polycrystalline nanoparticles (50 nm) with average crystalline size 4 nm [8].

[d] Nanoparticles with polycrystalline Co core of diameter 40 nm and Ag shell of thickness 28 nm [8].

[e] Nanoparticles prepared by sol-gel method. Average diameter is referenced in the brackets [7,9].

[f] Strongly interacting non-monodisperse nanoparticles of average diameter 5 nm [38].

$$\theta = \begin{cases} -(T - T_P)/(T_{r1} - T_P); T \leq T_P, \\ (T - T_P)/(T_{r2} - T_P); T > T_P \end{cases} \quad (2)$$

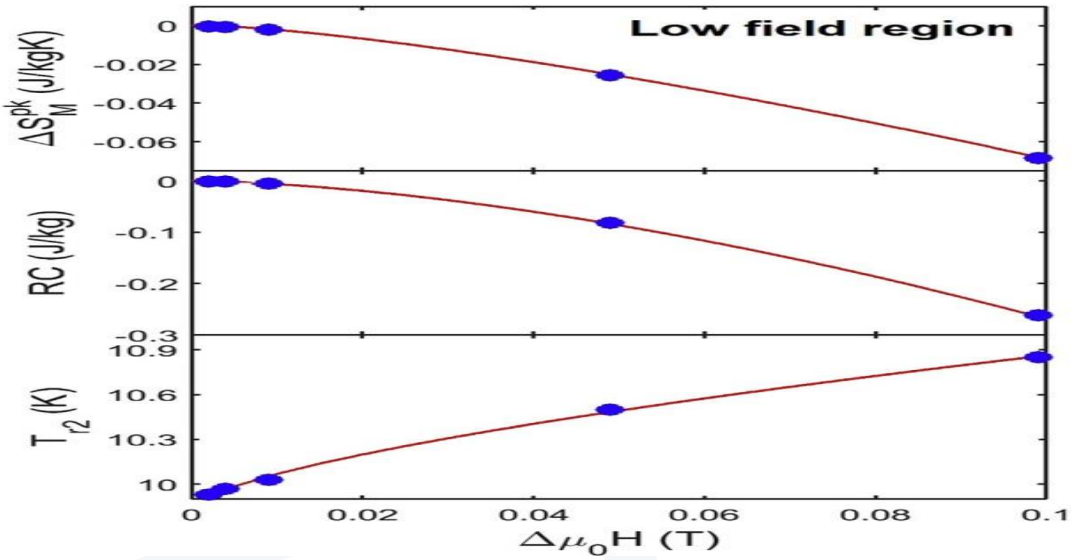


Fig. 4. Low field dependence of the peak magnetic entropy change, refrigerant capacity and reference temperature ($T_{r2}$) of Co/Au nanoparticle system.

Fig. 4 shows the collapse of $\Delta s_M$ (T, H) data (presented in the Fig. 3) onto universal curve constructed for the - $\Delta s_M$(T) maxima after employing scaling analysis according to Eq. (2). Analogous behavior has already been reported [24] in similar Co/Ag and Ni/Ag core/shell nanoparticle systems, where the surface spins freezing transition as typical order disorder transition was found as an origin of this behavior. Due to the existence of master curve, super spin glass freezing occurring in our Co/Au system resembles the features of the second order phase transition in the vicinity of $T_p$. The absence of thermal hysteresis in the ZFC/FC curves for fields above 1 T indicated a different nature of the transition, as can be observed in the absence of collapse of the rescaled

1 T curve onto the master curve for lower fields. In order to examine the phenomenon in more detail, further analysis of relevant magneto caloric parameters dependence on the magnitude of applied magnetic field change has been carried out. As it was reported [18], field dependence of $\Delta S_M^{pk}$, $T_r$. and refrigeration capacity (RC) can be utilized for the calculation of critical exponents which control magnetic phase transition at the proximity of critical temperature. Refrigeration capacity is the measure of the energy that can be transferred between the hot and cold reservoirs and is defined as [11]. In low and high applied magnetic fields. As we mentioned before, Franco et al. [24] studied similar systems of pure Co, Co/Ag and Ni/ Ag core/shell nanoparticles where surface spin freezing process at low temperatures was revealed. They established m= 1.47 from RC vs. ΔH dependence for field changes above 1 T and found out that this exponent did not vary with the change of core or shell material what points to the fact that the nature of the spin glass phase where ΔH is the difference between minimum and maximum applied fields.

$$RC(\Delta H) = \int_{T_{cold}}^{T_{hot}} \Delta S(T, \Delta H) dT, \qquad (3)$$

Usually, it is calculated as full width at half maximum of the $\Delta s_M(T)$ peak times the peak value $\Delta S_M^{pk}$ and in the case of SOPT, RC should obey scaling law [18] $RC - H^m, m = 1 + \frac{1}{\delta}$ shows RC (ΔH) dependence up to ΔH= 100 mT of investigated Co/Au nanoparticle system and fit of experimental data yielded the value of m = 1.68 from which $\delta = 1.47$ was calculated. It is necessary to emphasize that we excluded the values of $\Delta S_M^{pk}$, $T_r$ and RC obtained for the field change of 1 T from corresponding data fits. This was due to the absence of thermal hysteresis in $M^{ZFC}/M^{FC}$ curves at $\mu_0 H = 1T$, what indicates different behavior of the system transition is not altered by material characteristics. Since our value m =1.68 differs from the one determined for surface spin freezing, we suppose that transition between super paramagnetic and super spin glass state [39] at low applied fields is of distinct nature. Furthermore, the comparison of $\delta = 1.47$ determined for our Co/Au system with the value of $\delta = 3$ resulting from the mean-field theory [18] points to the fact that this theory is not suitable for the description of investigated SSG transition.

In the case of materials which do not follow a mean-field approach, the magnetic equation of state of such a material in the proximity of the transition temperature can be approximately described by the Arrott-Noakes equation of state [21,40].

$$H^{1/\gamma} = a(T - T_C)M^{1/\gamma} + bM^{1/\beta+1/\gamma} \quad (4)$$

where a, b are parameters of the equation, γ and β are the critical exponents. $T_C$ is the critical temperature represented by Curie temperature in standard SOPT. In our case, we attributed critical temperature $T_C$ to super spin glass freezing temperature $T_{SSG}$ ~7 K determined from magnetic AC susceptibility data analysis [25]. If we express field dependence as $\Delta S_M \sim H^n$ and consider the relationship $\beta + \gamma = \beta\delta$ (4) leads to relationship between the exponent n at the Curie point and the critical exponents of the material [41].

$$n = 1 + \frac{1}{\delta}(1 - \frac{1}{\beta}) \quad (5)$$

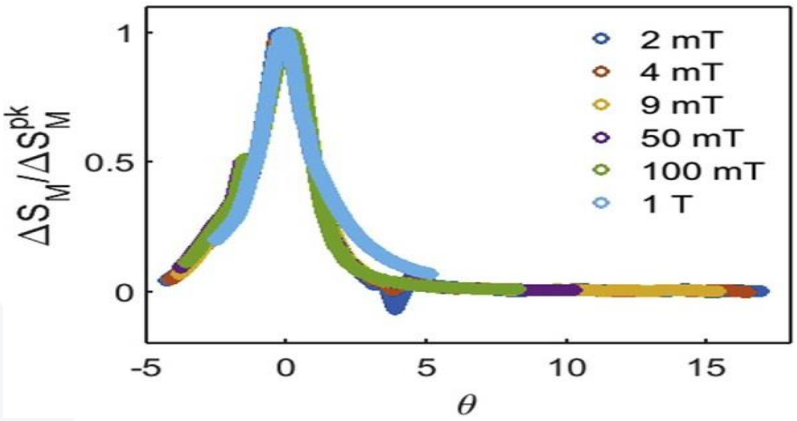


Fig. 5. The collapse of $\Delta S_M(T, \Delta H)$dependences onto single universal curve.

Fit of experimental $\Delta S_M^{pk}(\Delta H)$ data of investigated Co/Au nanoparticle system presented in Fig. 5 released the value of n = 1.29 and subsequently β = 1.73 and γ = 0.81 were calculated. Obtained values are in high discordance with the values characteristic of the mean field theory or Ising models, Table 2.

Table 2

Determined critical exponents.

| | β | γ | δ |
|---|---|---|---|
| Co/Au nanoparticles[a] | 1.73 | 0.81 | 1.47 |
| Mean field theory [18] | 0.5 | 1 | 3 |
| 3-d Ising model [42] | 0.31 | 1.25 | 4.82 |
| 2-d Ising model [42] | 0.13 | 1.75 | 15 |

[a] Exponents calculated for low applied magnetic fields.

The only critical exponent found in line with mean-field approach was σ = 0.65, that is related to critical exponents of the spontaneous magnetization at zero field ($M \sim (T_C - T)^b$, where $T_C$ is

the Curie temperature and $T < T_C$), and to the field dependence of magnetization at the Curie temperature($M \sim H^{1/d}$) via expression $\sigma = \beta\delta$ In our study, $\sigma$ was established employing $T_{r2} \sim H^{1/\sigma}$ fit to the experimental data [18].

Since no thermal hysteresis was observed in the Co/Au nanoparticle system for high applied fields (above 1 T), isothermal M (H) data were processed employing Eq. (1) for the evaluation of the systems' magneto caloric properties in high field region (analysis not shown in this work). Magnetic entropy change exhibited sharp peak at 7.5 K and its magnitude scaled with the applied field following power $\Delta S_M^{pk}(\Delta H) \sim H^{0.81}$, where the exponent was obtained by fitting the experimental data, Fig. 6. Apparently, magneto caloric response of the system qualitatively differs depending on low or high applied field magnitude. Due to very sharp $\Delta S_M$ peak character, insufficient experimental data hampered further scaling analysis as well as critical exponent's calculations. Nevertheless, our analysis of MCE revealed distinct behavior of Co/Au nano- particle system in low and high applied field regions and confirmed that examined transition from SPM to SSG state in low field region is of the second order type.

## Conclusions

Magneto caloric effect has been observed in Co/Au nanoparticle system exhibiting transition from super paramagnetic to super spin glass state. Decreasing the temperature below sufficiently low value, strong inter-particle interactions become dominant inducing collective behavior of nanoparticles' magnetic moments what results in the super spin frustration and non-equilibrium dynamics. Since magnetic characteristics of SSG state differ significantly from SPM state, abrupt change in magnetic entropy of the system was expected and experimentally confirmed. The values of $\left|\Delta S_M^{pk}\right| =$ 0.7 J/kgK and corresponding refrigeration capacity RC = 4.49 J/ kg have been established for applied field $\mu_0 H = 1T$. It has been shown that despite of evident thermal hysteresis of the system observed in low applied magnetic fields, universal curve can be constructed from $\Delta s_M(T, H)$ data recorded in field-cooling protocol.

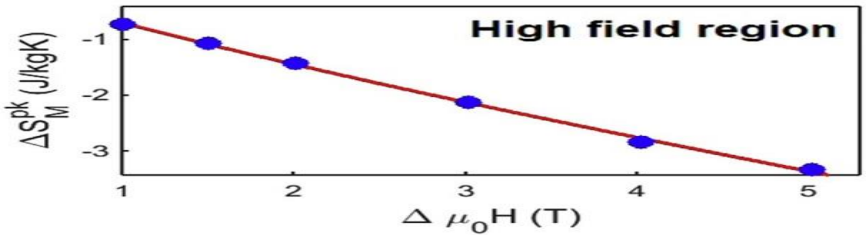


Fig. 6. High field dependence of the peak magnetic entropy change of Co/Au nano- particle system.

This suggests that the transition between super paramagnetic and super spin glass state evidenced in the system is of the second order (SOPT). Further data analysis by means of scaling laws valid for magnetic materials undergoing the second order phase transition revealed significant deviations of calculated critical exponents from the values typical of mean-field theory or Ising models what suggests that application of these approaches has limitations for examined transition description. Further, established exponents do not match with those reported for nanoparticle systems where freezing of surface spins into spin glass state proceeds. This indicates that there is a need of proposing new theory describing those processes in nanoparticle systems.

## References

1. Urinov, K. O., Jumanov, K. A., Khidirov, A. M., Urinov, S. K., Abdiyev, J. M., Jumaboyev, T. A., & Eshmirzayev, M. R. (2020, April). Magnetocaloric effect in polycrystalline cobalt. In Journal of Physics: Conference Series (Vol. 1515, No. 2, p. 022079). IOP Publishing.
2. Saidov, A. S., Saparov, D. V., Usmonov, S. N., Kutlimratov, A., Abdiev, J. M., Kalanov, M., ... & Akhmedov, A. M. (2021). Investigation of the Crystallographic Perfection and Photoluminescence Spectrum of the Epitaxial Films of (Si2) 1-x (GaP) x Solid Solution, Grown on Si and GaP Substrates with the Crystallographic Orientation (111). Advances in Condensed Matter Physics, 2021.
3. LEYDERMAN, A., Saidov, A. S., USMONOV, S., Abdiyev, J. M., & Suyarov, Q. T. (2021, February). INFLUENCE OF WEAK GRADED GAP ON INJECTION DIFFUSION REGIMES OF CURRENT TRANSPORT IN SEMICONDUCTOR PN-STRUCTURES. In Congress Dates (p. 40).
4. Raufovich, M. R., & Muzaffar o'g'li, A. J. (2022). THE ROLE OF TEACHER AND STUDENT COOPERATION IN THE MODERN EDUCATIONAL PROCESS OF GOOGLE DOCS. Web of Scientist: International Scientific Research Journal, 3(1), 579-589.

5. Abdiev, J., Safarov, O., & Julanov, H. (2022). Study of the properties of polymer composites–reinforcement based on glass and basalt fibers. Eurasian Scientific Herald, 7, 77-88.
6. Urinov, K. O., Jumanov, K. A., Khidirov, A. M., Urinov, S. K., Abdiyev, J. M., Jumaboyev, T. A., & Eshmirzayev, M. R. (2020). Magnetocaloric effect in polycrystalline cobalt. In Journal of Physics: Conference Series (Vol. 1515, p. 022079).
7. Urinov, K. O., Jumanov, K. A., Khidirov, A. M., Urinov, S. K., Abdiyev, J. M., Jumaboyev, T. A., & Eshmirzayev, M. R. (2020). Magnetocaloric effect in polycrystalline cobalt. In JOP Conference Series: Metrological Support of Innovative Technologies (pp. 22079-22079).
8. Urinov, K. O., Jumanov, K. A., Khidirov, A. M., Urinov, S. K., Abdiyev, J. M., Jumaboyev, T. A., & Eshmirzayev, M. R. (2020, April). Magnetocaloric effect in polycrystalline cobalt. In Journal of Physics: Conference Series (Vol. 1515, No. 2). IOP Publishing.
9. Urinov, K. O., Jumanov, K. A., Khidirov, A. M., Urinov, S. K., Abdiyev, J. M., Jumaboyev, T. A., & Eshmirzayev, M. R. (2020, April). Magnetocaloric effect in polycrystalline cobalt. In Journal of Physics Conference Series (Vol. 1515, No. 2, p. 022079).
10. Saidov, A. S., Saparov, D. V., Usmonov, S. N., Kutlimratov, A., Abdiev, J. M., Kalanov, M., ... & Akhmedov, A. M. (2021). Investigation of the Crystallographic Perfection and Photoluminescence Spectrum of the Epitaxial Films of (Si2) 1-x (GaP) x Solid Solution, Grown on Si and GaP Substrates with the Crystallographic Orientation (111). Advances in Condensed Matter Physics, 2021.
11. Bolkievna, I. A. LEARNING FROM UZBEK AND PERSIAN TRADITIONS: THE ROLE OF ENVIRONMENTAL PERCEPTIONS IN THE CREATION OF SPACE IS A GARDEN-CREATING PARADISE.
12. Saidov, A. S., Saparov, D. V., Usmonov, S., Kutlimratov, A., Abdiev, J. M., Kalanov, M., ... & Akhmedov, A. M. (2021). Investigation of the Crystallographic Perfection and Photoluminescence Spectrum of the Epitaxial Films of (Si 2) 1-x (GaP) x 0≤ x≤ 1 Solid Solution, Grown on Si and GaP Substrates with the Crystallographic Orientation (111). Advances in Condensed Matter Physics, 2021.
13. Saidov, A. S., Saparov, D. V., Usmonov, S. N., Kutlimratov, A., Abdiev, J. M., Kalanov, M., ... & Akhmedov, A. M. (2021). Investigation of the Crystallographic Perfection and Photoluminescence Spectrum of the Epitaxial Films of (Si2)(GaP) x (0≤ x≤ 1) Solid Solution, Grown on Si and GaP Substrates with the Crystallographic Orientation (111).

14. Saidov, A. S., Saparov, D. V., Usmonov, S. N., Kutlimratov, A., Abdiev, J. M., Kalanov, M., & Razzakov, A. S. (2021). Investigation of the Crystallographic Perfection and Photoluminescence Spectrum of the Epitaxial Films of (Si [sub. 2])[sub. 1-x](GaP)[sub. x](0≤ x≤ 1) Solid Solution, Grown on Si and GaP Substrates with the Crystallographic Orientation (111). Advances in Condensed Matter Physics, 2021.
15. Saidov, A. S., Saparov, D. V., Usmonov, S. N., Kutlimratov, A., Abdiev, J. M., Kalanov, M., ... & Akhmedov, A. M. (2021). Investigation of the Crystallographic Perfection and Photoluminescence Spectrum of the Epitaxial Films of (Si 2) 1-x (GaP) x 0≤ x≤ 1 Solid Solution, Grown on Si and GaP Substrates with the Crystallographic Orientation (111). Advances in Condensed Matter Physics.
16. LEYDERMAN, A. Y., SAIDOV, A., USMONOV, S. N., ABDIYEV, J., & SUYAROV, Q. (2021, February). INFLUENCE OF WEAK GRADED GAP ON INJECTION DIFFUSION REGIMES OF CURRENT TRANSPORT IN SEMICONDUCTOR PN-STRUCTURES. In Congress Dates (p. 40).
17. LEYDERMAN, A. Y., SAIDOV, A., USMONOV, S. N., ABDIYEV, J., & SUYAROV, Q. (2021, February). INFLUENCE OF WEAK GRADED GAP ON INJECTION DIFFUSION REGIMES OF CURRENT TRANSPORT IN SEMICONDUCTOR PN-STRUCTURES. In Congress Dates (p. 40).
18. Leiderman, A. Y., Saidov, A. S., & Abdiyev, J. M. (2021). INJECTION DIFFUSION PROCESSES IN THE WEAK LINEAR GRADED-BAND SEMICONDUCTOR pn-STRUCTURES. Euroasian Journal of Semiconductors Science and Engineering, 3(1), 3.
19. Leiderman, A. Y., Saidov, A. S., & Abdiyev, J. M. INJECTION DIFFUSION PROCESSES IN THE WEAK LINEAR GRADED-BAND SEMICONDUCTOR pn-STRUCTURES. Journal of Semiconductors, 3(1), 3.
20. Abdiev, J., Safarov, O., & Julanov, H. (2022). Study of the properties of polymer composites–reinforcement based on glass and basalt fibers. Eurasian Scientific Herald, 7, 77-88.
21. Abdiev, J., Safarov, O., & Julanov, H. Study of the properties of polymer composites–reinforcement based on glass and basalt fibers.
22. Abdiev, J., & Safarov, O. (2022). BASALT FIBER-BASIC (PRIMARY) CONCEPTS. Web of Scientist: International Scientific Research Journal, 3(4), 212-240.
23. Abdiev, J., & Safarov, O. BASALT FIBER-BASIC (PRIMARY) CONCEPTS.
24. KUŞÇULU, N. (2021). Congress Dates.

25. Abdiev, J., Safarov, O., & Julanov, H. (2022). Study of the properties of polymer composites–reinforcement based on glass and basalt fibers. Eurasian Scientific Herald, 7, 77-88.
26. Abdiev, J., Safarov, O., & Julanov, H. (2022). Study of the properties of polymer composites–reinforcement based on glass and basalt fibers. Eurasian Scientific Herald, 7, 77-88.
27. al-Khwarizmi, M., Abdullayeva, D. O. T., qizi Abdieva, N. M., & Khasanova, D. Y. DEVELOPMENT OF ALGORITHMS AND PROGRAMS FOR PROCESSING SPEECH SIGNALS ON VISUAL DSP++ PLATFORM.
28. Abdiev, J., Safarov, O., & Julanov, H. Study of the properties of polymer composites–reinforcement based on glass and basalt fibers.
29. al-Khwarizmi, M., Abdullayeva, D. O. T., qizi Abdieva, N. M., & Khasanova, D. Y. DEVELOPMENT OF ALGORITHMS AND PROGRAMS FOR PROCESSING SPEECH SIGNALS ON VISUAL DSP++ PLATFORM.
30. Bolkievna, I. A., & AbdievMuzaffar o'g'li, J. (2022). LEARNING FROM UZBEK AND PERSIAN TRADITIONS: THE ROLE OF ENVIRONMENTAL PERCEPTIONS IN THE CREATION OF SPACE IS A GARDEN-CREATING PARADISE. Web of Scientist: International Scientific Research Journal, 3(4), 188-211.
31. Bolkievna, I. A. LEARNING FROM UZBEK AND PERSIAN TRADITIONS: THE ROLE OF ENVIRONMENTAL PERCEPTIONS IN THE CREATION OF SPACE IS A GARDEN-CREATING PARADISE.
32. KUŞÇULU, N. (2021). Congress Dates.
33. Abdiev, J., & Safarov, O. BASALT FIBER-BASIC (PRIMARY) CONCEPTS.
34. KUŞÇULU, N. (2021). Congress Dates.
35. Xusanbek Ulug'bek o'g, M., al-Khwarizmi, M., Abdullayeva, D. O. T., qizi Abdieva, N. M., & Khasanova, D. Y. (2022, June). DEVELOPMENT OF ALGORITHMS AND PROGRAMS FOR PROCESSING SPEECH SIGNALS ON VISUAL DSP++ PLATFORM. In E Conference Zone (pp. 83-99).
36. KUŞÇULU, A. P. D. N. Access Date: 22.06. 2021.
37. Xusanbek Ulug'bek o'g, M., al-Khwarizmi, M., Abdullayeva, D. O. T., qizi Abdieva, N. M., & Khasanova, D. Y. (2022, June). DEVELOPMENT OF ALGORITHMS AND PROGRAMS FOR PROCESSING SPEECH SIGNALS ON VISUAL DSP++ PLATFORM. In E Conference Zone (pp. 83-99).
38. Xusanbek Ulug'bek o'g, M., al-Khwarizmi, M., Abdullayeva, D. O. T., qizi Abdieva, N. M., & Khasanova, D. Y. (2022, June). DEVELOPMENT OF ALGORITHMS AND PROGRAMS FOR PROCESSING SPEECH SIGNALS ON VISUAL DSP++ PLATFORM. In E Conference Zone (pp. 83-99).

39. Al-Khwarizmi, M., Abdullayeva, D. O. T., qizi Abdieva, N. M., & Khasanova, D. Y. DEVELOPMENT OF ALGORITHMS AND PROGRAMS FOR PROCESSING SPEECH SIGNALS ON VISUAL DSP++ PLATFORM.
40. Xusanbek Ulug'bek o'g, M., al-Khwarizmi, M., Abdullayeva, D. O. T., qizi Abdieva, N. M., & Khasanova, D. Y. (2022, June). DEVELOPMENT OF ALGORITHMS AND PROGRAMS FOR PROCESSING SPEECH SIGNALS ON VISUAL DSP++ PLATFORM. In E Conference Zone (pp. 83-99).
41. al-Khwarizmi, M., Abdullayeva, D. O. T., qizi Abdieva, N. M., & Khasanova, D. Y. DEVELOPMENT OF ALGORITHMS AND PROGRAMS FOR PROCESSING SPEECH SIGNALS ON VISUAL DSP++ PLATFORM.
42. Abdullayeva, D. O. T., Ismoilov, M. M., qizi Abdieva, N. M., & Khasanova, D. Y. (2022). Peach signal control software is an important part of our lives. Eurasian Scientific Herald, 7, 145-152.
43. Abdullayeva, D. O. T., Ismoilov, M. M., qizi Abdieva, N. M., & Khasanova, D. Y. (2022). Peach signal control software is an important part of our lives. Eurasian Scientific Herald, 7, 145-152.
44. Taylanov, N. A. (2022). A Fourth-Order Runge-Kutta Method for Numerical Solution of the Kuramoto-Sivashinsky Equation. Eurasian Scientific Herald, 7, 58-61.
45. Taylanov, N. A. (2022). A Fourth-Order Runge-Kutta Method for Numerical Solution of the Kuramoto-Sivashinsky Equation. Eurasian Scientific Herald, 7, 58-61.
46. Abdurazzokovich, N., Xudoyor o'g'li, S., & Muzaffar o'g'li, J. A Fourth-Order Runge-Kutta Method for Numerical Solution of the Kuramoto-Sivashinsky Equation.
47. Abdiev, J., Abdieva, N. M., & Khasanova, D. Y. (2022). Physical Terms, Problems and Their Solutions. Problems and Their Solutions (March 25, 2022).
48. Ortikovich, U. J., Muzaffar o'g'li, A. J., & Rafikovich, M. R. **Fex V**3– x **04**MAGNETIC AND ELECTRICAL PROPERTIES OF SPINEL.
49. Ortikovich, U. J., Muzaffar o'g'li, A. J., & Rafikovich, M. R. **Fex V**3– x **04**MAGNETIC AND ELECTRICAL PROPERTIES OF SPINEL.
50. KUŞÇULU, N. (2021). Congress Dates.
51. KUŞÇULU, N. (2021). Congress Dates.
52. KUŞÇULU, N. (2021). Congress Dates.